

Automatic Detection of Pathological Myopia using Variational Level Set

N.M. Tan, J. Liu, D.W.K. Wong, J.H. Lim, Z. Zhang, S. Lu, H. Li, S.M. Saw, L. Tong, T.Y. Wong

Abstract— Pathological myopia, the seventh leading cause of legal blindness in United States, is a condition caused by pathological axial elongation and eyes that deviates from the normal distribution curve of axial length, resulting in impaired vision. Studies have shown that ocular risks associated with myopia should not be underestimated, and there is a public health need to prevent the onset or progression of myopia. Peripapillary atrophy (PPA) is one of the clinical indicators for pathological myopia. In this paper, we introduce a novel method, to detect pathological myopia via peripapillary atrophy feature by means of variational level set. This method is a core algorithm of our system, PAMELA, an automated system for the detection of pathological myopia. The proposed method has been tested on 40 images from Singapore Cohort study Of the Risk factors for Myopia (SCORM), producing a 95% accuracy of correct assessment, and a sensitivity and specificity of 0.9 and 1 respectively. The results highlight the potential of PAMELA as a possible clinical tool for objective mass screening of pathological myopia.

Index Terms: Pathological Myopia, Peripapillary Atrophy (PPA), Level set.

I. INTRODUCTION

MYOPIA is a vision condition with the inability to see objects at a distance clearly. Pathological myopia, also known as high myopia or degenerative myopia is commonly defined as having a spherical equivalent (SE) of at least -6.0 diopters (D) [1]. This ocular disease is the seventh leading cause of blindness in adults in the United States [2], is present in about 0.5% of the general population in Europe [3] and is estimated to represent 2% of all types of myopia [4]. In Singapore, Hong Kong and Taiwan, the prevalence of this disease appears to be on the rise [5]-[6]. In ocular pathology, the retinal changes in high myopia people includes peripapillary atrophy (PPA), peripheral lattice degeneration, tilting or malinsertion of the optic disc, posterior staphyloma, and breaks in Bruch's membrane [5]-[6].

As patients with high myopia are more prone to ocular abnormalities, it is increasingly essential to manage the

progression of degenerative myopia with early detection and treatment. Current clinical practices of detecting pathological myopia rely heavily on the manual screening and efforts of the clinicians. As such, the PAMELA (PAthological Myopia dETECTION through peripapillary Atrophy) system seeks to provide an automatic means for mass screening of pathological myopia.

In this paper, we present a fast and novel method in the PAMELA system to detect pathological myopia in fundus images using variational level set. This method, known as the disc difference approach, detects two main areas: the optic disc with PPA and the fundamental optic disc. The difference in the two areas provides a visual cue for potential PPA regions. The contextual differences of these regions are further analyzed to determine the existence of PPA. Pathological Myopia can then be inferred from this symptom. To the best of our knowledge, there are no reports of a similar system that automatically detects pathological myopia using peripapillary atrophy.

II. METHODS

Our method is based on the approach to detect pathological myopia through the presence of peripapillary atrophy (PPA). PPA is the receding of the retinal pigment epithelium around the optic nerve head. It is a clinical indicator and a useful feature as it is visually present in fundus images.

The framework of the proposed disc difference method, Fig. 1, consists of 3 main components: Optic Disc Identification, Optic Disc Extraction and PPA Analysis. The optic disc identification module performs a search for possible optic disc regions to isolate and form a Region of Interest (ROI) for the system's core algorithm. Next, the optic disc extraction module applies variational level set on the optic disc internally to locate the contour of the optic disc. The variational level set algorithm is then extended to the outer region of the optic disc to establish the possible PPA areas that may exist in the region closely surrounding the optic nerve head. These PPA areas are investigated in the PPA analysis module with a knowledge-based constraint to evaluate if there is a presence of PPA. As a result, this indicates if pathological myopia is detected.

Manuscript received April 7, 2009.

N.M. Tan, J. Liu, D.W.K. Wong, J.H. Lim, Z. Zhang, S. Lu and H. Li are with the Institute for Infocomm Research, A*STAR, Singapore (phone: (065)6408-2489; fax (065)6776-1378; e-mail: nmtan@i2r.a-star.edu.sg.

S.M. Saw is with the Singapore Eye Research Institute and the Department of Epidemiology and Public Health, National University of Singapore.

L. Tong is with the Singapore National Eye Center and the National University of Singapore

T.Y. Wong is with the Singapore Eye Research Institute and the National University of Singapore.

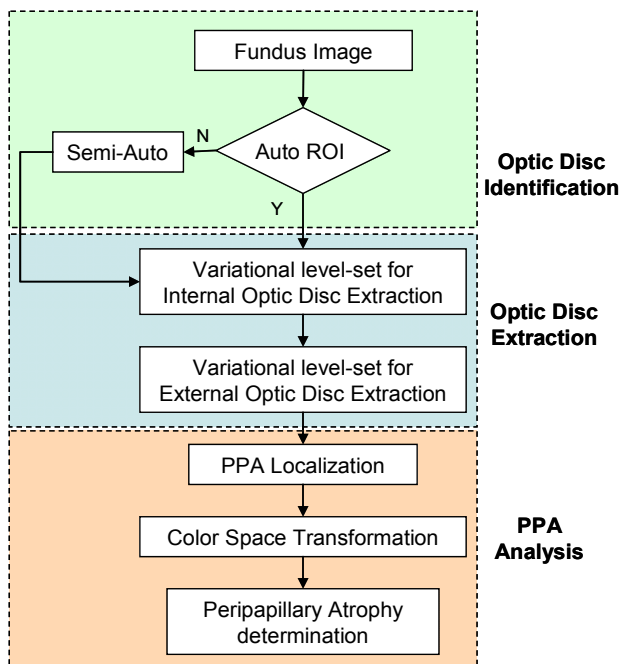


Fig. 1. Disc Difference Framework

A. Optic Disc Identification

From prior work, the optic disc can first be identified and localized by the highest 0.5% of pixel intensity in a composed lattice from a given fundus image, as described in [7]-[8]. The resultant ROI is a 800 by 800 image which helps to save computational resources for faster processing and analysis.

As the fundus images in the dataset can contain other visual ocular degenerating features that may result in an inaccurate ROI, we have included a semi-auto mode to our method to detect the optic disc via interactive user input of the optic disc centre. In the event of an inaccurate ROI detection, the user can click on the center of the optic disc to provide the correct ROI. This allows us to test the method extensively. Fig. 2 shows the ROI selection after automatic optic disc identification on a right eye fundus image.

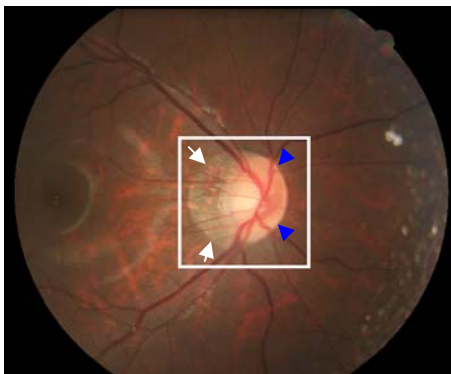


Fig. 2. Optic Disc Identification with ROI enclosed in white box. Note the PPA region (white arrowheads) is the pigmented half beside the optic disc (blue arrows).

B. Optic Disc Extraction

Once the ROI is determined, we apply variational level set inside and outside of the optic disc for internal and external optic disc extraction. As compared to traditional level set formulations, the variational level set function by Li et al[9] can be initialized as functions which are computationally faster to generate than the signed distance function. Furthermore, the proposed algorithm is able to segment weak boundaries robustly.

We initialized the variational level set algorithm as proposed by Li et al [9], with a horizontal ellipse within and a vertical ellipse outside the optic disc. We utilized a horizontal ellipse internally in order to bypass and reduce the influence of the edges of the retinal vessels and allow the level set function to grow and seek for the correct optic disc boundary. Conversely, a vertical ellipse is set externally as it best represents the physiological shape of the optic disc. An example is presented in Fig. 3.

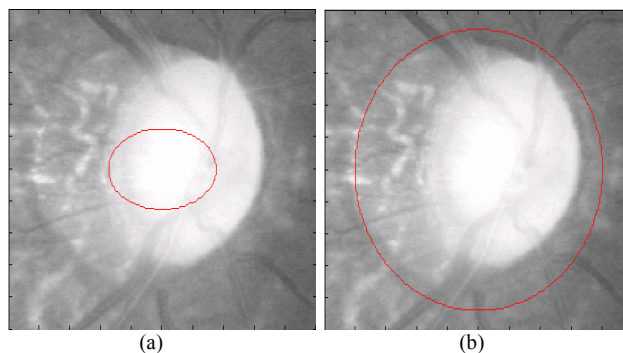


Fig. 3. (a) Initial level set contour for internal optic disc extraction, (b) Initial level set contour external optic disc extraction.

From our experiments, we found that working on the red channel of the image is optimal as it gives the best description about the edge gradient of the optic disc and PPA.

The proposed total energy functional (1), by Li et al [9], consists of a penalizing energy (2) and an external energy (3). The penalizing energy is an expression to distinguish and compensate the distance between the level set function(ϕ) from the signed distance function. This expression maintains the level set function as an approximate signed distance function automatically during evolution, removing the need for costly re-initialization, while the external energy (3) directs the motion of the level set towards the object features.

$$\varepsilon(\phi) = \mu P(\phi) + \varepsilon_{g,\lambda,v}(\phi) \quad (1)$$

$$P(\phi) = \int_{\Omega} \frac{1}{2} (|\nabla \phi| - 1)^2 dx dy \quad (2)$$

$$\varepsilon_{g,\lambda,v}(\phi) = \lambda L_g(\phi) + v A_g(\phi) \quad (3)$$

$$L_g(\phi) = \int_{\Omega} g\delta(\phi)|\nabla\phi|dxdy \quad (4)$$

$$A_g(\phi) = \int_{\Omega} gH(-\phi)dxdy \quad (5)$$

$$g = \frac{1}{1+|\nabla G_{\sigma} * I|^2} \quad (6)$$

where

ϕ is the level set curve;

μ determines the deviation of ϕ from the signed distance function;

$L_g(\phi)$ is the weighted length of the zero level curve;

$A_g(\phi)$ is the weighted area inside the zero level curve;

$\lambda > 0$ and ν are the constants of $L_g(\phi)$ and $A_g(\phi)$.

The minimized gradient flow equation in (7) can be expressed as (8)

$$\frac{\partial\phi}{\partial t} = -\frac{\partial\varepsilon}{\partial\phi} \quad (7)$$

$$\frac{\partial\phi}{\partial t} = \mu \left[\Delta\phi - \text{div} \left(\frac{\nabla\phi}{|\nabla\phi|} \right) \right] + \lambda\partial(\phi)\text{div} \left(g \frac{\nabla\phi}{|\nabla\phi|} \right) + \nu g\delta(\phi) \quad (8)$$

where

Δ is the Laplacian operator;

t is the time step for the iteration.

The constant of the weighted area inside the level curve, ν , is forced to be negative when the initial contour is placed inside of the optic disc for fast expansion of the level set energy. Similarly, ν is constrained to be positive when we apply the level set algorithm for external optic disc extraction.

The time step is set at $t = 5$ with 500 iterations for the internal disc extraction. As the edges of the PPA region are weak, we limit the evolution of the externally applied level set to 300 iterations and maintain $t = 5$ for stable level set evolution.

The final evolution of the gradient flow results in an approximate boundary of the optic disc (R1) and a region containing both the optic disc and PPA (R2). Fig. 4 shows the boundary contours of R1 and R2. It is important to note that though a larger time step gives a faster evolution, the accuracy in the boundary location would be compromised.

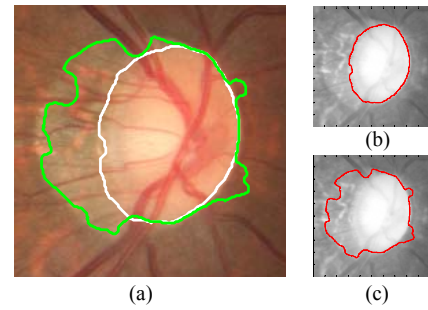


Fig. 4. (a) R1(white) and R2(green) superimposed on ROI, (b) Final evolution of internal optic disc extraction after 500 iterations, (c) Final evolution of external optic disc extraction after 300 iterations

C. PPA Analysis

The optic nerve head is typically divided into four sectors: Superior, Inferior, Temporal and Nasal. An example is shown in Fig. 5. It is important to note that the nasal and temporal zones are of opposite sides if it was a left eye image. As PPA is known to often occur in the temporal sector, we apply a knowledge-based constraint mask to focus the detection in these sectors.

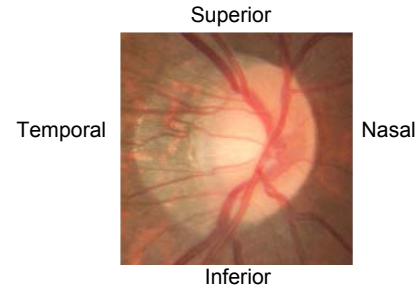


Fig. 5. Clinically defined sectors for the optic nerve head.

The potential PPA regions, R_p , are first derived from the difference of the regions R1 and R2. The left quadrant mask (Fig. 6(a)) and right quadrant mask (Fig. 6(b)) are then applied onto the region R_p . Figs. 6(c) and 6(d) show the results after employing the constraint masks

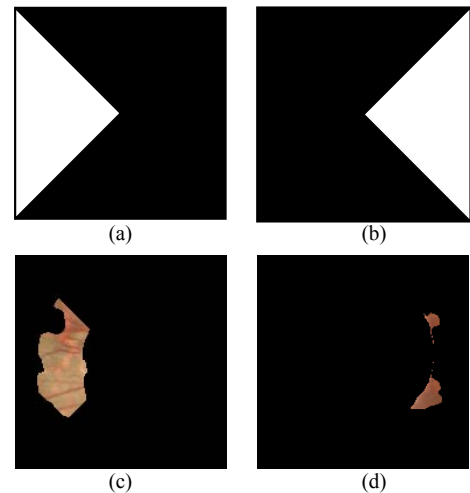


Fig. 6. (a) Left Quadrant Constraint Mask, (b) Right Quadrant Constraint Mask, (c) Right Quadrant Residue, (d) Left Quadrant Residue

The color space of the quadrant residues (Figs. 6(c) and 6(d)) is transformed from RGB to HSV color model. Using a threshold in the hue layer, we are able to segment the PPA from the quadrant residues. The hue component is used as it describes the color of the image without the effects of intensity.

It is noticed that some of the retinal images contain retinal nerve fiber striations. The nerve fiber layer is one of the innermost layers within the retina. This layer can be seen as a number of faint stripes that fan or diffuses out from the optic nerve in a radial-like pattern against the background formed by the retinal pigment epithelium and the underlying blood vessels of the choroid.

We reduce the false detection caused by these patterns by taking the absolute difference between the areas in the detected candidate regions of the Right and Left Quadrants. If the difference is large, this gives an indication that the remains in the temporal half have a distinctly dissimilar surface. This implies that PPA is detected.

III. EXPERIMENTS AND RESULTS

We evaluated the PAMELA system on 40 images from the Singapore Cohort study Of the Risk factors for Myopia (SCORM). This is a 10 years on-going cohort study conducted since 1999 on school children aged 7 to 9 years. All the subjects in the study had retinal photography performed by trained staff using the Canon CR6-45NM Non-Mydriatic Retinal Camera. The fundus images were taken with the eyes centered on the disc and macular. Our test set ground truth consists of 20 images from individual subjects who are clinically diagnosed with pathological myopia along with the presence of peripapillary atrophy(PPA) and 20 images of subject individuals with clinically normal eyes.

TABLE I
STATISTICS OF THE OBTAINED RESULTS

Image Category	# of samples	# of correct detection	# of false detection	Accuracy
Normal	20	20	0	100%
Pathological Myopia	20	18	2	90%
Total	40	38	2	95%

The test set was processed in the automatic mode of the PAMELA system, achieving an accuracy of 95% with sensitivity of 90%, and specificity of 100%. The results show that our proposed method is able to detect pathological myopia via PPA accurately for both normal and pathological myopic cases.

We analyzed the failure images and found that the problems occur when the optic disc is not contained within the centre of the ROI. This causes the level set algorithm to have a false estimation of the PPA region. However, when the images were subsequently processed with a user-defined ROI, as discussed in Section II, the system was able to accurately determine the presence of PPA.

IV. CONCLUSION

Pathological myopia, which is often accompanied by peripapillary atrophy (PPA), is a frequently under-estimated yet rapidly increasing global health concern. In this paper, we have introduced a novel technique, disk difference approach, to automatically detect this ocular disease via retinal photography. The disk difference method applies a combination of variational level set and knowledge constraints to detect PPA. The method has been validated on 40 images from the SCORM database with very encouraging results, attaining an accuracy of 95% with low false detection errors. The high sensitivity and specificity makes this a viable approach for automatic mass screening of pathological myopia. This method is a core function within the PAMELA system. Further work in PAMELA could include fusion of other image processing algorithms and techniques and testing on larger datasets.

REFERENCES

- [1] Y.F. Shih, T.C. Ho, C.K. Hsiao, L.L.-K. Lin, "Visual outcomes for high myopic patients with or without myopic maculopathy: a 10 year follow up study," *Br. J. Opth*, 90, 546-550. 2006.
- [2] National Society for the Prevention of Blindness. NSFB Fact Book: Estimated Statistics for the Prevention of Blindness, 1966; 44.
- [3] Strömberg E. Über Refraktion und Achsenlänge des menschlichen Auges, *Aca Ophthalmol* 1936; 14:281-93.
- [4] Michaels DD. *Visual Optics and Refraction; A Clinical Approach*, 2nd ed. St Louis: CV Mosby, 1980; 513.
- [5] Saw SM, Katz J, Schein OD, Chew SJ, Chan TK. Epidemiology of myopia. *Epidemiol Rev.* 1996;18:175-187.
- [6] T. Curtin BJ. *The Myopias: Basic Science and Clinical Management*. Philadelphia: Harper & Row; 1985.
- [7] J. Liu, D.W.K. Wong, J.H. Lim, H. Li, N.M. Tan, Z. Zhang, T. Y Wong, R. Lavanya, "ARGALI : An Automatic Cup-To-Disc Ratio Measurement System For Glaucoma Analysis Using Level-Set Image Processing", 13th International Conference on Biomedical Engineering (ICBME2008), 2008.
- [8] J. Liu, D.W.K. Wong, J.H. Lim, H. Li, F. Yin, X. Jia, K.L. Chan, N.M. Tan, T.Y. Wong, "ARGALI-an Automatic cup-to-disc Ratio measurement system for Glaucoma detection and AnaLysis framework", *Proceedings of SPIE*, Vol. 7260, 72603K (2009)
- [9] C. Li, C. Xu, C. Gui, M.D. Fox, "Level Set Evolution Without Re-initialization: A New Variational Formulation", *Proc. of the 2005 IEEE Computer Society Conference on Computer Vision and Pattern Recognition*, 2005.